MRS2015 / 6th International Workshop on Magnetic Resonance

Imaging shallow water bearing structures using three dimensional magnetic resonance tomography with separated loops

Jiang Chuandong
College of Instrumentation & Electrical Engineering, Jilin University Changchun, 130026, China
Chuandongjiang@gmail.com

Mike Müller-Petke
Leibniz Institute for Applied Geophysics Hannover, D-30655, Germany
Mike.Mueller-Petke@liag-hannover.de

Lin Jun
College of Instrumentation & Electrical Engineering, Jilin University Changchun, 130026, China
lin_jun@jlu.edu.cn

Ugur Yaramanci
Leibniz Institute for Applied Geophysics Hannover, D-30655, Germany
ugur.yaramanci@liag-hannover.de

SUMMARY

The technique of surface NMR has been applied to image 1D, 2D and recently 3D sub-surface structures. While limited resolution is reported for imaging deep 3D structures using a coincident loop configuration, high resolution is obtained for shallow 2D structures by including separated loop configurations. We adapt the concept of separated transmitter and receiver loops to obtain increasing resolution for imaging 3D shallow structures. We present a numerically efficient approach to calculate the 3D kernel with sufficient accuracy but small number of elements. Using synthetic data, we show that including separated loop layouts enhances 3D image reconstruction. To evaluate our 3D inversion approach, a field campaign including surface NMR with various layouts and GPR measurements was conducted on top of a frozen artificial barrier lake in the Harz Mountains (Germany, Lower Saxony) with a well-known geometry. We show that results obtained from measurements using the coincident loop layout gives a rough approximation of the lakes bathymetry while including separated loop layouts provides an more detailed view into the subsurface. In particular, the obtained image match not only the known water content of 100%, but the geometry known from construction plans and estimated from ground penetration radar profiles. In addition to the 3D assessment, a 2D profile is extracted from the 3D data set to demonstrate the need for 3D inversion.

Key words: Hydrogeophysics, Surface NMR, Modelling, Inversion, Tomography

INTRODUCTION

Surface nuclear magnetic resonance (surface NMR) is a relatively new geophysical technique that provides direct quantitative information about the spatial location and amount of water in the subsurface (i.e., water not bound to minerals or water in solid phase) (Legchenko et al., 2002). In most applications, surface NMR is used for one-dimensional (1D) depth sounding using a coincident transmitter and receiver loop and is referred to as magnetic resonance sounding (MRS). The application of surface NMR to 2D targets is commonly referred to as magnetic resonance tomography (MRT). Surface NMR including separated transmitter and receiver loops has been applied to enhance spatial resolution capabilities (Hertrich et al., 2009) at shallow depths. Concerning 3D implementation, surface NMR was reported for the first time by Legchenko et al. (2011), and successfully used to investigate accumulated water within the Tete Rousse glacier (French Alps) (Legchenko et al., 2014), all of which combining overlapping 1D coincident loop soundings to a 3D data set. It is common to all presented 3D inversion approaches to use very large and regular cells in the model domain (20 m × 20 m × 5 m) that are justified by limited resolution capabilities when targeting deep structures down to about 80 m.

We apply the idea of separated transmitter and receiver loops in order to increase the resolution of 3D MRT when targeting shallow water bearing structures. Although separated loop layouts are used for 2D imaging, it is the first time applied for a 3D investigation. Thus, we evaluate the resolution capabilities including separated loops in comparison to a coincident loop survey using a 3D synthetic study. Next, we conducted a comprehensive 3D MRT survey on a frozen artificial barrier lake built in the Harz Mountains (Germany, Lower Saxony), which not only provides a known water content, but a known geometry from the construction plans. This well-defined object gives a unique opportunity to verify the modelling and inversion approach for 3D MRT.

METHOD AND RESULTS

3D Kernel function

The magnetic field distribution in the subsurface is to be calculated first. We calculate the transmitter and receiver fields in the subsurface using a commercial finite element code (COMSOL). For a given subsurface model, mesh generators for tetrahedral elements have become more popular. For instance, for our kernel calculations we typically divide the subsurface into two region as shown in Fig. 1. The primary region is for the coverage area of the transmitter and receiver loops on the surface and down to a certain depth using relatively fine meshes. The surrounding region is extend to few hundred meters from the edge faces of the primary region and contains very coarse meshes with maximum sizes up to hundred meters. The surrounding region ensures minimizing any boundary effect of the magnetic field calculation.

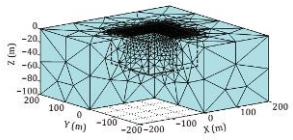

Figure 1. 3D mesh as used for kernel calculation

After deriving the magnetic fields, co-and counter rotation components and projections to the Earth's field are calculated.

The kernel value $G(\mathbf{r}_e, q)$ at a single node uses the NI form (hammer integration)

$$\int G(\mathbf{r}_e, q)\,\mathrm{d}^3\mathbf{r}_e = V_e \sum_{i=1}^{N} W_i G_i\left(\zeta_1^i, \zeta_2^i, \zeta_3^i, \zeta_4^i, q\right) \qquad (3)$$

where $\mathbf{r}_e$ and V_e is the spatial position and volume of an element e, W_i are weights and $\left(\zeta_1^i, \zeta_2^i, \zeta_3^i, \zeta_4^i\right)$ are tetrahedral coordinates of an evaluation point i. We use NI of the order of five, i.e., we use $N = 15$ evaluation points that provide an exact solution if G_i can be approximated by a polynomial of degree 5 or less.

In order to evaluate the quality of the kernel calculation implementing NI of the order five is compared to a kernel calculated using a refined tetrahedron mesh. Comparing a simulation using the coarse mesh without NI (Fig. 2b) shows that the absolute error to the reference (Fig. 2a) is significant as the oscillation of the kernel are not sufficiently sampled. Implementing NI reduced the absolute error to less than 10 nV, i.e. the deviation is in the order of 1%. We therefore consider the NI method using 15 evaluation points to be as accurate as the calculation based on the refined mesh using 27 additional elements. This result is due to the optimal distribution of evaluation points applying the theory of numerical integration compared to a non-optimal distribution using simple refinement.

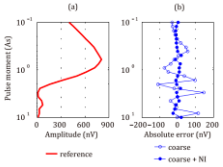

Figure 2. Simulation of the 3D MRT forward response for the different meshes

Synthetic example

As we hypothesize that implementing separated loop configuration into a 3D field layout increases shallow lateral resolution, a synthetic study is designed to compare two loop configurations as shown in the Figure 3.

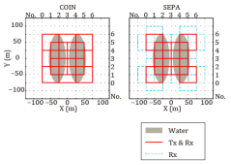

Figure 3. MRT layouts using only the coincident loop (a) and including the separated loops (b).

One (COIN) uses thirteen transmitter and coincident receiver loop positions with an overlapping as reported by Legchenko (2011) and the other one (SEPA) bases on only nine transmitter but 9×5 receiver positions thus including separated loop layouts. Both layouts cover the investigation area of 75×75 m^2. For modeling, we used an Earth's magnetic field of B_0 =48967 nT at an inclination of I =60° and an declination of D =47° E. Subsurface resistivity is homogeneous and set to 300 Ωm and 20 pulse moments are distributed logarithmically between 0.1 As and 10 As. Two ellipsoid bodies of 50% water content embedded in a try surrounding and characterized by their semi-principal axes lengths of a =75 m, b =20 m, and c =15 m; located at z =-15 m, y =0 m, and x =±30 m define the underlying model. The two ellipsoids are very close to each other, the minimum distance is only 10 m, thus this model allows for evaluating the resolution capabilities of the two layouts. Synthetic signal are contaminated with 20 nV Gaussian noise. The estimated models as given is Figure 4 provide a data fit of rms =19.68 nV and rms =20.07 nV for COIN and SEPA, respectively, i.e. satisfy the data within the noise level.

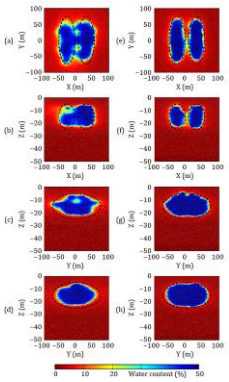

Figure 4. Inversion results for COIN (a-d) and SEPA (e-f).

Figure 4a/e shows horizontal slices at the depth of 15 m. It shows that for SEPA the position and shape are reconstructed, the two ellipsoids are well resolved, and the maximum water content is estimated as 51.50 %. For the COIN survey the approximate shape and position of the targets is estimated, but the two ellipsoids cannot be resolved as separated units. For the vertical slice at y =0 m presented in the Figure 2b/f, the result is similar. While SEPA allows for identifying the two structures as separated units, the COIN survey does not provide sufficient lateral resolution. The two vertical slices at x =±30 m (Figure 4c/g and 4d/f) show only slight differences.

In particular, the improvement is remarkable as the enhance resolution is from the increasing receiver loops, instead of additional transmitter positions. The coincident loop configuration requires more transmitting measurements, and thus results in more field time, assuming multi-channel instrumentation and sufficient field capabilities. The separated loop configuration employs more receiver loops to provide the enhanced resolution. Less transmitter positions are used, therefore field time is conserved.

Experimental results

A field campaign for a 3D MRT data set was carried out at the upper Einersberger Lake (Harz Mountains, Germany) in the winter of 2010. The Einersberger Lake is an artificial barrier lake built for energy supply. The lake was chosen mainly due to the well-known geometry from the construction plans. Beside these plans, the bathymetry is additionally provided by the ground penetrating radar (GPR) measurements. A 1D MRS survey in the middle of the lake found three water layers: 1) the Ice layer 0-0.35 m depth, 2) the bulk water layer 0.35-7.45 m depth and 3) hard rock basement below 7.45~m. Both, MRS (at the single point) and GPR confirm the information on the construction plan.

Given this well-known object, we decided to verify 3D MRT at this site. The main goal was to image the lake volume and evaluate the estimated water content. The 3D MRT measurements were carried out using the separated loop configuration of four 50×50 m^2 square loops in each transmitter position (Figure 5). This configuration is similar to the synthetic example, but beside the one coincident loop, deploys only three receiver loops (Figure 4 legend) as we were limited by four receiver channels of GMR instrument at that time. To cover the whole area, nine transmitter positions were selected, Tx11, Tx22, Tx33, Tx44, Tx55, Tx15, Tx24, Tx42, and Tx51, and for each transmitter position, three additional receiver loops (using three out of four directions) allowing to image the lake. For instance, the receiver loops for Tx11 are Rx12, Rx01, and Rx10, although Rx21 is missing, we expected that the information of the subsurface water can be obtained by the loop layout at Tx22 which contains Rx21 as a receiver loop. Therefore, the combination of nine separated loops should allow for resolving the water body of the lake in approximate 100×100 m^2 area.

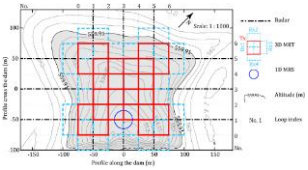

Figure 5. Field setup for 3D MRT and the GPR.

The complete MRT data set consists of 36 sounding curves each with 24 pulse moments, corresponding to nine transmitters and four receivers. The pulse length was 10 ms and q ranges between 0.1 and 10 As. The stacking rate was 16. The data error of the initial values is calculated as 32 nV from the mono-exponential fitting, taking the extrapolation into account. For the kernel calculation, the temperature of the lake is set at 275 kelvins. The water conductivity was measured as 300 Ωm, the variations of which will have no influence on the kernel function for conductivities over 100 Ωm. The Earth's magnetic field was 48985 nT, corresponding to the Larmor frequency of 2058.8 Hz and the variations during the course of the survey was below 0.5 Hz.

The inverse modeling has been carried out using IVI scheme. The lower boundary for the water content is set to zero, while the upper boundary is set to 1.1. The regularization parameter is chosen to satisfy the data within the estimated data error and to obtain a smooth model. The obtained rms-deviation between estimated and observed data is 36 nV.

The known structure of the lake is given as the cyan mesh in the Figure 4. Three horizontal slices from the estimated water distribution at 2 m, 4 m and 6 m depth are shown. The model shows a water content up to 100 %, primarily accumulated in the central part of lake. Outside the lakes boundaries the water content decreases close to zero, thus imaging the try hard rock.

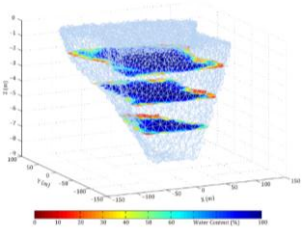

Figure 6. Estimated 3D water content distribution of the Einersberger Lake.

In addition to the three horizontal sections, six vertical slices of the estimated water distribution as well as the geometry as from the construction plan, and provided by GPR measurements are shown in Figure 7 allowing for a more detailed discussion. Firstly, GPR results nicely confirm the geometry obtained from the construction plans, only a little differences are visible at the bottom of the lake. The MRT result is in a good agreement with the lake geometry. At the central parts the water content is about 100 %. Outside the lake, the water content is almost close to zero. Close to the sharp boundaries of the lake, the water content image shows a rather smooth transient to zero and in particular relatively low water content. We identified two main reasons for low water content at the boundaries: (i) incomplete coverage of the lake by the MRT layout and (ii) insufficient resolution to image sharp boundaries. The six slices show, that the bottom boundary is better resolved compared to the lateral extend of the lake. Especially the shallow and thin bank of the lake (e.g. slice at y=50 m) are rather unresolved. We expect additional transmitter position should allow for improved imaging. Further differences are present for the slice at x=50 m at the bottom close to x=-50 m. While MRT displays low water content, neither GPR nor the construction plan indicate the hard rock boundary. This remains an open question.

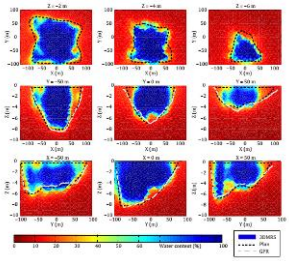

Figure 7. The water content distribution of nine sections from the 3D surface MRT result using SEPA.

In order to compare images as derived from a COIN survey with a SEPA survey (as we did in the synthetic study) a COIN data set is extracted from the complete data set and inverted for the water content distribution (Fig. 8) with the same parameters as used for SEPA. Generally, the results from COIN, in contrast to the SEPA results, show a smoother and more compact body of water, in which the central water content is about 100% as well, and outside is close to zero. The boundaries of the lake are less consistent with the construction plan and GPR. In particular this is because only the central part of the lake is well covered with loop positions, thus resulting in lower lateral resolution of the lakes boundaries. One can significantly find water outside the lake boundary in x<0 m, and lack of water at the bottom of the lake below z=-6 m. Although the results from the SEPA survey (Fig. 5) does contain few artifacts with low water content, a 3D MRT survey including separated loop soundings provides a superior image of the lakes geometry compared to a COIN survey. Note that the SEPA survey does not include more transmitter position, hence, does not take more measurement time.

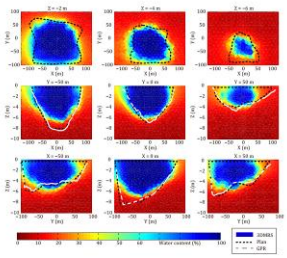

Figure 8. The water content distribution of nine sections from the 3D surface MRT result using COIN.

In addition to the comparison of the 3D results, 2D MRT data sets are extracted to evaluate the need for 3D inversion. We expect that, a 2D image inverted from a 2D data set in 3D conditions will show artifacts. We decided for the x=-50 m line as a GPR measurements is present at this line and because 3D conditions are expected for this profile. Unfortunately, as for the Tx13 position no transmitter loop is present, we decided to include the Tx24 and Tx22 that are not in-line. However, otherwise the loop coverage would be too bad to conduct a realistic comparison. In summary we used Tx11, Tx22, Tx24 and Tx15 for COIN and include Rx10(Tx11 as the transmitter), Rx11(Tx11), Rx12(Tx11 and Tx22), Rx14(Tx24), Rx15(Tx15) and Rx16(Tx16) for SEPA. Finally, we obtain the water content from the 2D MRT data sets (Fig. 12) using a 2D kernel (Hertrich et al., 2009). Essentially, the results confirm our hypothesis. The slice from the 3D MRT survey using the SEPA layout matches the GPR and lake geometry best. The 2D SEPA image (Fig. 9d) does not show a homogeneous water body but fluctuation in the water content indicating a non-existing structure. The 2D MRT COIN image does not show these fluctuating water content and the result is similar to that is obtained in 3D for the COIN layout. However, resolution is low, represented by a lack of water content, at the lakes edges because of missing loop coverage. We assume that the fluctuation are smoothed out due to the lower resolution. The water below the bottom of the lake is overestimation due to the information from the middle lake at x>-50 m.

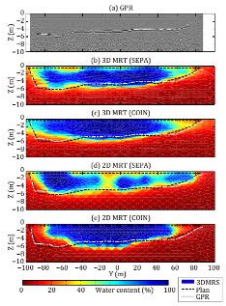

Figure 9. The water content distribution of one GPR profile from the 3D and 2D surface MRT result using COIN and SEPA.

CONCLUSIONS

Given the presented results of the synthetic study and the field case, incorporating separated transmitter and receiver (SEPA) configuration leads to an enhanced image resolution for shallow three dimensional structures. Consequently, we extend the conclusions published for 2D (Hertrich et al., 2009) to 3D cases. As the SEPA layout includes additional receiver but keep the number of transmitter position, the total measurement time remains constant. However, we note that adding receiver loops may sometimes be difficult, e.g. in rough terrain or areas difficult to access.

As known for most geophysical techniques and using the field case we demonstrate that images obtained from 2D MRT data measured on substantially 3D subsurface condition suffer from artifacts. It remains an open question for further research to quantify what is substantially 3D.

At the time of the field measurements, only four receiver channels were available limiting the number of separated receiver. Considering the studies of 2D MRT we expect additional benefit by implementing not only half-overlapping configuration but edge-to-edge separation. Moreover, the number of receiver channels limited the number of direction to place the receiver loop relative to transmitter. It is subject to further research which and how many direction are reasonable and how different layout impact on the resolution of the derived image.

As recently shown, implementing an inversion scheme that incorporates the relaxations times, such as the QT inversion, will improve both image quality and geological interpretation. Furthermore, new transmitter loop layouts together with receiver arrays (Jiang et al., 2015) increased field progress for 2D investigation. We expect similar developments for 3D layouts.

ACKNOWLEDGMENTS

We like to thank the Raphael Dlugosch and Robert Meyer for acquiring the surface NMR and Jan Igel and Dieter Epping for measuring the GPR data.

REFERENCES

Hertrich, M., 2008, Imaging of groundwater with nuclear magnetic resonance: Progress in Nuclear Magnetic Resonance Spectroscopy, 53, 227-248.

Hertrich, M., A. G. Green, M. Braun, and U. Yaramanci, 2009, High-resolution surface-NMR tomography of shallow aquifers based on multi-offset measurements: Geophysics, 74, G47-G59.

Legchenko, 412 A., and P. Valla, 2002, A review of the basic principles for proton magneticresonance sounding measurements: Journal of Applied Geophysics, 50, 3-19.

Legchenko, A., M. Descloitres, C. Vincent, H. Guyard, H. Garambois, K. Chalikakis, and M. Ezersky, 2011, Three-dimensional magnetic resonance imaging for groundwater: New Journal of Physics, 13, 025022.

Müller-Petke, M., R. Dlugosch, and U. Yaramanci, 2011, Evaluation of surface nuclear magnetic resonance-estimated subsurface water content: New Journal of Physics, 13, 095002.